

## Analysis of Differential and Total Cross-Section Data for High-Energy $p\bar{p}$ and $p\bar{p}$ Interactions

WOLFGANG DRECHSLER\* AND ROBERTO SUAYA†

*Stanford Linear Accelerator Center, Stanford University, Stanford, California 94305*

(Received 15 June 1970)

An analysis of  $p\bar{p}$  and  $p\bar{p}$  data in terms of a  $K$ -matrix model for the Pomeranchuk exchange and the absorptive corrected  $P'$  and  $\omega$  Regge-pole contributions is presented. The model provides a quantitative understanding of high-energy  $p\bar{p}$  and  $p\bar{p}$  total cross-section measurements and the measured ratio of the real to the imaginary part of the  $p\bar{p}$  elastic forward scattering amplitude. The structure observed in  $(d\sigma/dt)_{p\bar{p}}$  around  $t = -0.8$  GeV<sup>2</sup> and in  $(d\sigma/dt)_{pp}$  at  $t = -1.2$  GeV<sup>2</sup>, the shrinkage patterns in both differential cross sections, and the crossover phenomenon are explained in the framework of this model.

### I. INTRODUCTION

IN a recent publication,<sup>1</sup> a  $K$ -matrix model for the Pomeranchuk exchange contribution to high-energy elastic scattering and diffraction dissociation processes has been proposed which is confronted in this paper with differential and total cross-section measurements for high-energy  $p\bar{p}$  and  $p\bar{p}$  collisions. The main feature of the proposed model for Pomeranchuk exchange is that the vacuum exchange contribution is thought to originate from multiple exchange of various lower-lying trajectories, having an intercept  $\alpha(0) = 0.5$  and a slope  $\alpha' = 1$  GeV<sup>-2</sup>, accompanied by the formation of a sequence of intermediate excited states (resonances) of the colliding particles. The model at the present stage does not account for spin-flip contributions. It can be regarded as a unitarized relativistic multiple-scattering model for spinless incoming and outgoing particles. In terms of  $j$ -plane singularities, the proposed interpretation of the vacuum exchange contribution corresponds to a superposition of cuts in the complex angular momentum plane. However, the number of parameters describing the Pomeranchuk contribution is two, as in the conventional Pomeranchuk pole model.

The amplitudes for elastic scattering and diffraction dissociation processes are written down in the impact-parameter language<sup>2</sup> neglecting spin and isospin, and are made unitary by a multichannel  $K$ -matrix parametrization assuming an effective two-particle description for the inelastic states in the unitarity relations. The attractive features of this model for the Pomeranchuk contribution are that it predicts (a) logarithmic shrinkage of diffraction peaks up to very high energies corresponding to an effective Pomeranchuk pole of slope  $(\alpha_P')_{eff} = \frac{1}{2}\alpha'$ , in agreement with the recent measurements from Serpukhov,<sup>3</sup> and (b) a logarithmic approach to asymptotic conditions for total cross sections similar to other multiple-scattering approaches to the vacuum

exchange contribution.<sup>4</sup> Furthermore, a natural explanation for the crossover phenomenon is provided in terms of absorptive corrections to the input Regge Born terms. We shall show below that the model is, moreover, able to reproduce the structure in the  $p\bar{p}$  differential cross section at  $t \approx -1.2$  GeV<sup>2</sup> and in the  $p\bar{p}$  differential cross section between  $t = -0.6$  and  $-0.9$  GeV<sup>2</sup>. However, we find that the present spinless treatment is unable to account for  $(d\sigma/dt)_{p\bar{p}}$  beyond  $t = -2$  GeV<sup>2</sup>. We are inclined to attribute this observation to non-negligible spin-flip contributions being present at momentum transfer larger than  $|t| = 2$  GeV<sup>2</sup>, where the  $p\bar{p}$  differential cross section at  $p_{lab} = 19.2$  GeV/ $c$  has gone down by nearly five orders of magnitude compared to the value at  $t = 0$ .

### II. MODEL

In this section we collect the relevant formulas partly derived in Ref. 1. In the equations written below, the upper sign refers to  $p\bar{p}$  scattering whereas the lower sign refers to  $p\bar{p}$  scattering. Besides the diffractive contribution, we take only  $P'$  and  $\omega$  exchange in the  $t$  channel into account. Possible small  $\rho$ ,  $A_2$ ,  $\pi$ , or  $B$  contributions are neglected.<sup>5</sup>

The differential cross section and the optical theorem read

$$\frac{d\sigma}{dt} = \frac{1}{4\pi q^2 s} |f(s, t)|^2, \quad (1)$$

$$\text{Im} f(s, t=0) = \frac{1}{2} q(\sqrt{s}) \sigma_{tot}(s), \quad (2)$$

with

$$f(s, t) = 2\pi s \int_0^\infty b db \eta(b, s) J_0(b\sqrt{-t}), \quad (3)$$

\* Work supported in part by the U. S. Atomic Energy Commission and the Max Kade Foundation.

† Fellow from the University of Buenos Aires.

<sup>1</sup> W. Drechsler, Phys. Rev. D **1**, 364 (1970).

<sup>2</sup> R. Blankenbecler and M. L. Goldberger, Phys. Rev. **126**, 766 (1962).

G. G. Beznogikh *et al.*, Phys. Letters **30B**, 274 (1969).

<sup>4</sup> S. Frautschi and B. Margolis, Nuovo Cimento **56A**, 1155 (1968); C. B. Chiu and J. Finkelstein, *ibid.* **57A**, 649 (1968).

<sup>5</sup> The reason for this is that the  $pn$  charge-exchange reaction, which is expected to be dominated by isovector exchange, has a very small cross section at high energies. Moreover, these trajectories couple to the spin-flip amplitudes which we consistently neglect in this analysis.

where

$$\eta(b,s) = \frac{iC(b,s) - D(b,s)}{1 + C(b,s) + iD(b,s)} + [N^{P'}(b,s) \pm N^\omega(b,s)] \frac{1 - C(b,s) - 2iD(b,s)}{[1 + C(b,s) + iD(b,s)]^2}. \quad (4)$$

Here  $s$  is the total energy squared and  $q = \frac{1}{2}(s - 4m_p^2)^{1/2}$  is the relative momentum, with  $m_p$  denoting the proton mass.  $C(b,s)$  and  $D(b,s)$  in Eq. (4) are given by

$$C(b,s) = Q(s)e^{-b^2/2\rho}, \quad D(b,s) = R(s)e^{-3b^2/4\rho}, \quad (5)$$

where  $\rho = \alpha' \ln(s/s_0)$ , and<sup>6</sup>

$$Q(s) = \frac{\sigma_{\text{tot}}(\infty)}{8\pi\alpha' \ln(s/s_0)}, \quad R(s) = \frac{\tau}{8\pi\alpha' \ln(s/s_0)}. \quad (6)$$

The quantities  $N^{P',\omega}(b,s)$  represent the Fourier Bessel transforms of the single Regge exchange terms  $g^{P',\omega}(s,t)$ , for  $P'$  and  $\omega$  exchange, respectively, which are defined in Eq. (13) below. In Eq. (6),  $\alpha'$  is the slope of the particle trajectories which generate the Pommeranchuk contribution via multiple exchange and resonance excitation in the above described way. In the derivation of Eq. (4) it was assumed in Ref. 1 that  $s$  is large and that the real part of the diffractive contribution, measured by  $D(b,s)$ , is small compared to the imaginary part determined by  $C(b,s)$ . Separating the real and imaginary parts in Eq. (4) and neglecting terms of order  $[\tau/\sigma_{\text{tot}}(\infty)]^2$ , one obtains, besides a vacuum contribution to  $\text{Im}\eta(b,s)$  and  $\text{Re}\eta(b,s)$ , an absorptive correction to the input Regge-pole terms at impact parameter  $b$  and total energy squared  $s$  determined by the functions  $A(b,s)$  and  $B(b,s)$  [compare the second term in Eqs. (8) and (11) below] which are given by

$$A(b,s) = 4 \frac{R(s)e^{-3b^2/4\rho}}{[1 + Q(s)e^{-b^2/2\rho}]^3}, \quad (7)$$

$$B(b,s) = \frac{1 - Q(s)e^{-b^2/2\rho}}{[1 + Q(s)e^{-b^2/2\rho}]^2}.$$

We finally write down the expression for the total cross sections and the ratio of the real to imaginary part of the elastic forward scattering amplitudes in the  $K$ -matrix model for Pommeranchuk exchange:

$$\sigma_{\text{tot}}(s) = \sigma_{\text{tot}}^{P'}(s) + \frac{4\pi\sqrt{s}}{q} \times \left[ \int_0^\infty b db \{ \text{Im}[N^{P'}(b,s) \pm N^\omega(b,s)] B(b,s) - \text{Re}[N^{P'}(b,s) \pm N^\omega(b,s)] A(b,s) \} \right]. \quad (8)$$

<sup>6</sup> The connection between  $\tau$  and  $D$ , introduced in Ref. 1, is  $\tau = D/8\pi^2\alpha'^2 s_0^2$ .

Here the Pommeranchuk contribution to the total cross section is given by

$$\sigma_{\text{tot}}^{P'}(s) = \frac{4\pi\alpha'\sqrt{s}}{q} \ln \frac{s}{s_0} \ln \left[ 1 + \frac{\sigma_{\text{tot}}(\infty)}{8\pi\alpha' \ln(s/s_0)} \right]. \quad (9)$$

For extremely high energies the right-hand side of Eq. (9) approaches the constant value  $\sigma_{\text{tot}}(\infty)$ , which was the reason for having introduced this constant in Eq. (6). The value of  $\tau$  is related in a simple manner to the ratio of the real to the imaginary part of the elastic forward scattering amplitude for both  $pp$  and  $p\bar{p}$  at infinite energies according to

$$\lim_{s \rightarrow \infty} \frac{\text{Re}f(s, t=0)}{\text{Im}f(s, t=0)} = \xi(\infty) = -\frac{2}{3} \frac{\tau}{\sigma_{\text{tot}}(\infty)}. \quad (10)$$

At nonasymptotic  $s$ , one finds

$$\xi(s) = \frac{\text{Re}f(s, t=0)}{\text{Im}f(s, t=0)} = \xi(s) + \frac{4\pi\sqrt{s}}{q\sigma_{\text{tot}}(s)} \times \left[ \int_0^\infty b db \{ \text{Re}[N^{P'}(b,s) \pm N^\omega(b,s)] B(b,s) + \text{Im}[N^{P'}(b,s) \pm N^\omega(b,s)] A(b,s) \} \right], \quad (11)$$

where  $\sigma_{\text{tot}}(s)$  is given by Eq. (8) and  $\xi(s)$  is given by

$$\xi(s) = -\frac{2}{3} \frac{\tau}{\sigma_{\text{tot}}(s)} \left( \frac{s}{s - 4m_p^2} \right)^{1/2} \int_0^1 \frac{dx}{[1 + Q(s)x^{2/3}]^2}, \quad (12)$$

which, for  $s \rightarrow \infty$ , tends to the constant limit (10).

### III. ANALYSIS OF $pp$ AND $p\bar{p}$ DATA

We first determined a fit to the data for  $\sigma_{\text{tot}}^{pp}(s)$ ,  $\sigma_{\text{tot}}^{p\bar{p}}(s)$ , and  $\xi^{pp}(s)$ .<sup>7</sup> As input Regge-pole terms we used the following  $P'$  and  $\omega$  contributions:

$$g^{P'}(s,t) = -\frac{1}{2}(1 + e^{-i\pi\alpha_{P'}(t)})\beta_{P'}(s/s_0)\alpha_{P'}(t), \quad (13)$$

$$g^\omega(s,t) = -\frac{1}{2}(1 - e^{-i\pi\alpha_\omega(t)})\beta_\omega(s/s_0)\alpha_\omega(t),$$

where  $\beta_{P'}$  and  $\beta_\omega$  are supposed to be constants and  $\alpha_{P',\omega}(t) = \alpha_{P',\omega}(0) + t$ . Notice that in order to allow a Fourier-Bessel transformation to be made, we have assumed a certain ghost-eliminating mechanism being operative to remove the poles of the factor  $1/\sin\pi\alpha(t)$  appearing in the usual Regge-pole expressions. In Ref. 1 we introduced a weaker ghost-eliminating mechanism which was called "minimal ghost elimination" there, being different for positive- and negative-signature trajectories. To fit the total cross-section data and in particular the relatively weak  $s$  dependence of

<sup>7</sup> W. Galbraith *et al.*, Phys. Rev. **138**, B913 (1965); K. J. Foley *et al.*, Phys. Rev. Letters **19**, 857 (1967); IHEP-CERN Collaboration, Phys. Letters **30B**, 500 (1969).

$\sigma_{tot}^{pp}(s)$ , which comes about through a cancellation of the  $P'$  and  $\omega$  contributions, it turned out, however, that the minimal ghost-eliminating mechanism is not tenable and Eqs. (13) had to be used as input.

The fit obtained, using the program MINFUN of Berkeley-SLAC, had a  $\chi^2$  of 24.7 for 41 data points and seven parameters, and is shown by the curves labelled I in Figs. 1(a) and 1(b). The energy dependence of the total cross sections is well represented. The resulting values for the parameters are

$$(I) \quad \begin{aligned} \sigma_{tot}(\infty) &= 119.8 \text{ GeV}^{-2}, \\ \alpha_{P'}(0) &= 0.58, \quad \beta_{P'} = 79.8, \\ \alpha_{\omega}(0) &= 0.42, \quad \beta_{\omega} = 54.3, \\ \tau &= -20.4 \text{ GeV}^{-2}, \quad s_0 = 0.421. \end{aligned}$$

The curve labelled  $P$  in Fig. 1(a) corresponds to the Pomeranchuk contribution alone. The above value of  $\sigma_{tot}(\infty)$  of 46 mb coincides with the result obtained by Barger and Phillips<sup>8</sup> in fitting their cut model to essentially the same data. Observe, however, that these authors introduce *in addition* to a Pomeranchuk pole a cut contribution which turns out to require a negative coefficient. In our  $K$ -matrix approach such a contribution is automatically contained in the Pomeranchuk term. Furthermore, the real part of the vacuum contribution comes out to be negative and small compared

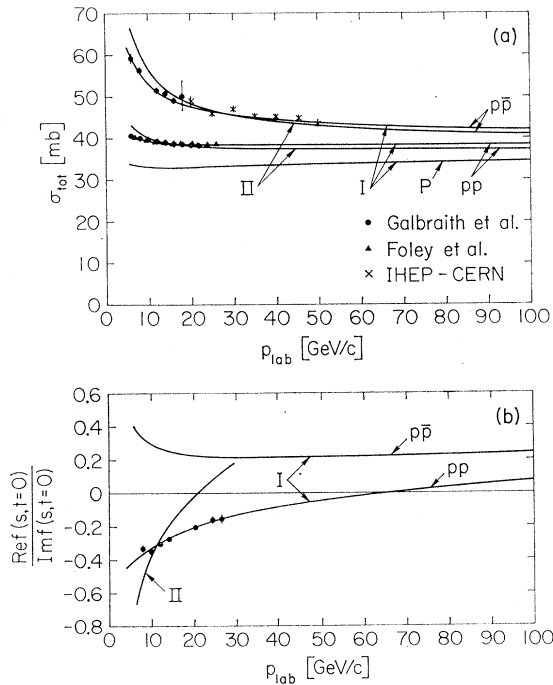


FIG. 1. Fit to (a) total cross sections and (b) ratio of real to imaginary part at  $t=0$  of Ref. 7. I: Solution I ( $P$ , Pomeranchuk contribution alone); II: Solution II.

<sup>8</sup> V. Barger and R. J. N. Phillips, Phys. Rev. Letters 24, 291 (1970).

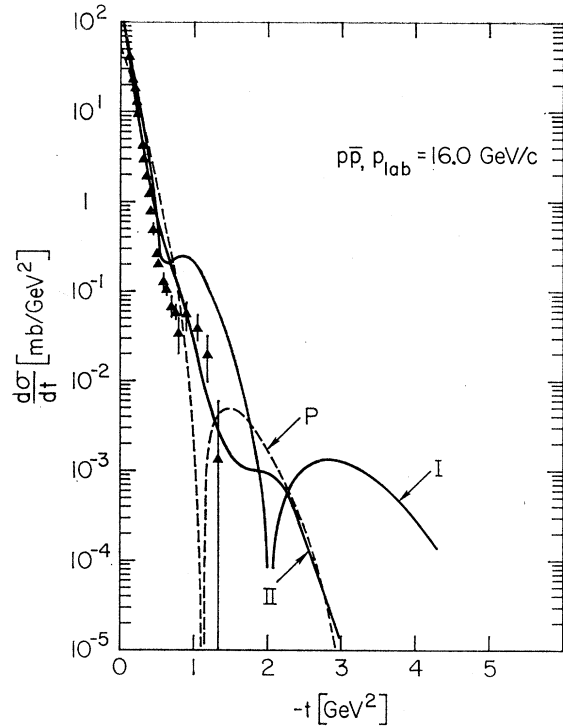


FIG. 2. Comparison with the  $p\bar{p}$  data of Ref. 11 at  $p_{lab}=16 \text{ GeV}/c$ . I: Solution I; II: Solution II ( $P$ , Pomeranchuk contribution alone).

to the imaginary part.<sup>9</sup> The ratio  $\text{Re}f(s, t=0)/\text{Im}f(s, t=0)$  for  $pp$  is predicted to change sign at about  $p_{lab}=60 \text{ GeV}/c$ . The asymptotic value of  $\xi^{pp}(s)$  and  $\xi^{p\bar{p}}(s)$  is  $\xi(\infty) = +0.11$ .

We now used the Solution I to make a prediction for the  $pp$  and  $p\bar{p}$  differential cross sections and compared it with the  $pp$  data at 10.94, 12.0, and 12.4  $\text{GeV}/c$  and the  $p\bar{p}$  data at 11.8 and 12.0  $\text{GeV}/c$ .<sup>10</sup> The model provided a reasonable prediction for  $t$  values in the range  $0 \leq |t| \leq 0.6 \text{ GeV}^2$  although the theoretical values corresponding to the above parameters come out in the low- $t$  range in both cross sections systematically somewhat bigger than the experimental values. The crossover of the predicted curves occurs at  $t = -0.20 \text{ GeV}^2$ , i.e., exactly where the experimental crossover of  $(d\sigma/dt)_{pp}$  and  $(d\sigma/dt)_{p\bar{p}}$  appears at this energy. This result differs from the one obtained in Ref. 1 (and also in Ref. 7) because of the different ghost-eliminating mechanism involved, as required by the fit to the total-cross-section data and the real to the imaginary part of the forward scattering amplitude. The striking feature of the calculation for  $(d\sigma/dt)_{p\bar{p}}$  with the parameters I is the dip-bump structure which appears between

<sup>9</sup> Remember that terms of order  $[\tau/\sigma_{tot}(\infty)]^2$  were neglected throughout.

<sup>10</sup> K. J. Foley *et al.*, Phys. Rev. Letters 15, 45 (1965); J. Or ear *et al.*, Phys. Rev. 152, 1162 (1966); K. J. Foley *et al.*, Phys. Rev. Letters 11, 503 (1963); D. Harting *et al.*, Nuovo Cimento 38, 60 (1965).

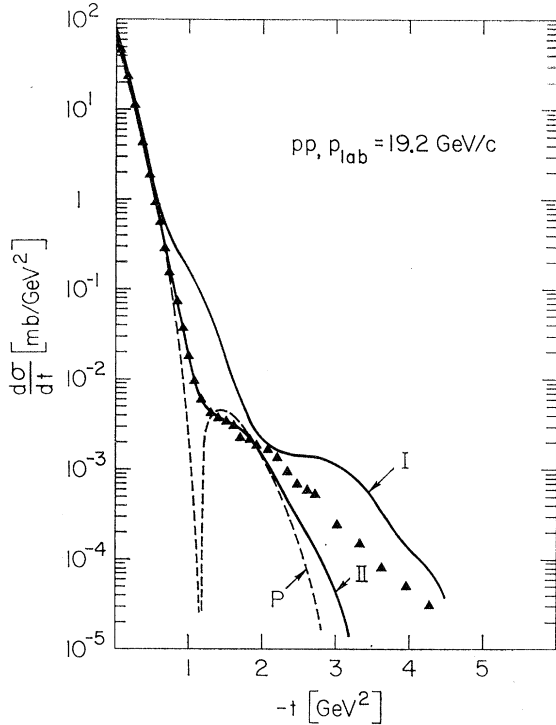


FIG. 3. Comparison with the  $pp$  data of Ref. 11 at  $p_{\text{lab}}=19.2$  GeV/c. I: Solution I; II: Solution II ( $P$ , Pomeranchuk contribution alone).

$-t=(0.6-0.9)$  GeV<sup>2</sup>. The structure is similar to the one shown in Fig. 2, curve I, corresponding to  $p_{\text{lab}}=16.0$  GeV/c, showing that this type of interference phenomenon producing structure in differential cross sections persists to rather large energies.

To determine the energy dependence of the diffraction peaks in this model, we repeated the described comparison at somewhat higher energies, i.e., at  $p_{\text{lab}}=16.0$  GeV/c for  $p\bar{p}$  and at  $p_{\text{lab}}=19.2$  GeV/c for  $pp$ .<sup>11</sup> The agreement in the interval  $0 \leq |t| \leq 0.6$  GeV<sup>2</sup> was slightly better, although the prediction still lies systematically above the experimental points. The general structure of the theoretical curves corresponding to Solution I is the same as at the lower energies and is shown by the curves labelled I in Figs. 2 and 3. In going from 12 to 16 GeV/c, the model predicted a small but noticeable amount of antishrinkage for  $(d\sigma/dt)_{p\bar{p}}$ , whereas no appreciable shrinkage in the  $pp$  case could be detected between 12 and 19.2 GeV/c.

We now made a search for a combined solution for  $(d\sigma/dt)_{pp}$  at 19.2 GeV/c,  $(d\sigma/dt)_{p\bar{p}}$  at 16 GeV/c,  $\sigma_{\text{tot}}^{pp}(s)$ ,  $\sigma_{\text{tot}}^{p\bar{p}}(s)$ , and  $\xi^{pp}(s)$ . The main problem consisted in estimating how far out in  $t$  our spinless model could be used to represent the data. After some numerical tests, we finally decided to limit the  $t$  range and to include only those experimental points for elastic

$pp$  scattering with  $|t| \leq 2.0$  GeV<sup>2</sup>. The obtained fits are shown by the curves labelled II in Figs. 1-3. The values for the parameters for the combined fit are

$$\begin{aligned} \sigma_{\text{tot}}(\infty) &= 118.6, \\ \alpha_{P'}(0) &= 0.38, & \beta_{P'} &= 64.9, \\ \alpha_{\omega}(0) &= 0.34, & \beta_{\omega} &= 53.1, \\ \tau &= -7.64 & s_0 &= 0.082; \end{aligned}$$

$\sigma_{\text{tot}}(\infty)$  is essentially unchanged compared to Solution I;  $\tau$  is considerably smaller and we lose the good description of  $\xi^{pp}(s)$  obtained before. We show by the curves labelled  $P$  in Figs. 2 and 3 the Pomeranchuk contribution to the differential cross sections. To first order in  $\tau$  these curves are independent of  $\tau$ .<sup>12</sup> As is clear from Fig. 3, the shoulder of the  $pp$  differential cross section at  $t=-1.2$  GeV<sup>2</sup> comes out very nicely in this model and is due to the vanishing of the Pomeranchuk contribution at this point. The  $K$ -matrix model predicts the vanishing of the Pomeranchuk term (diffraction zero) to move towards smaller values of  $|t|$  in a logarithmic fashion as the energy is increased.

#### IV. DISCUSSION

Comparing the set of values I and II, we observe (a) that Solution II is closer to exchange degeneracy for  $P'$  and  $\omega$ , which has a bearing on the shrinkage pattern as will be discussed below, and (b) that  $s_0$  in Solution II is considerably smaller. Such a small value of  $s_0$  is required in order to obtain a diffraction peak extending over four orders of magnitude. It is well known that changing the value of  $s_0$  to  $s_0 < 1$  corresponds to the introduction of residues decaying exponentially with  $t$ . The differential cross section is naturally very sensitive to changes in  $s_0$ . Total cross sections, on the other hand, are less sensitive to such changes since the residues can always be readjusted in certain limits without altering the goodness of the fit to both total and differential cross sections.

We have examined the interference between the Pomeranchuk term and the absorptive corrected  $P'$  and  $\omega$  contributions, behaving like  $1/\sqrt{s}$ , in order to determine the energy dependence of the diffraction cone in  $pp$  and  $p\bar{p}$  scattering, i.e., the shrinkage or antishrinkage at the present energies. It turns out that the following situation is realized in this model. For  $(d\sigma/dt)_{pp}$  the  $\omega$  contribution subtracts from the Pomeranchuk term for  $|t|$  smaller than the crossover point ( $t_{c.o.} \approx -0.20$  GeV<sup>2</sup>) and adds for  $|t|$  bigger than the crossover point. The reverse is true for the  $P'$  contribution. In a completely exchange-degenerate situation, the  $P'$  and  $\omega$  contributions cancel in the imaginary part of the amplitude and the energy behavior of the  $pp$  forward differential cross section shows as a result

<sup>11</sup> D. Birnbaum *et al.*, Phys. Rev. Letters **23**, 663 (1969); J. V. Allaby *et al.*, Phys. Letters **28B**, 67 (1968).

<sup>12</sup> The dependence of  $d\sigma/dt$  on  $\tau$  comes about through the absorptive correction of the  $P'$  and  $\omega$  contributions.

(disregarding the effect of the real part) the shrinkage pattern of the Pomanchuk term alone. The same is true if  $P'$ - $\omega$  exchange degeneracy in the residues and trajectories is only slightly broken as in our Solution II. For  $p\bar{p}$  scattering, however, both Regge pole contributions of order  $1/\sqrt{s}$  add below the crossover point and subtract beyond it, which makes the diffraction peak on the one hand steeper in  $p\bar{p}$  compared to  $pp$  and on the other hand expanding due to the *decaying* of the contributions of order  $1/\sqrt{s}$  in going to higher energies. Finally, however, at sufficiently high energies also the  $p\bar{p}$  differential cross section will show shrinkage according to  $(\alpha_{P'})_{\text{eff}} = \frac{1}{2}\alpha'$  as the  $pp$  diffraction peak does. The structure in  $(d\sigma/dt)_{p\bar{p}}$  around  $t = -0.8 \text{ GeV}^2$ —being an effect of the lower lying trajectories—is predicted to disappear with increasing  $s$ , whereas the shoulder in

$(d\sigma/dt)_{pp}$  at  $t = -1.2 \text{ GeV}^2$  is connected to the Pomanchuk contribution and will in this model develop into a more profound diffraction minimum with growing energy. We point out, however, that the curves labelled  $P$  in Figs. 2 and 3 do not represent asymptotic curves for the differential cross sections at large  $s$  but possess themselves a logarithmic energy dependence. This is implied by the statement that diffraction peaks shrink indefinitely in this model as  $s$  increases.

#### ACKNOWLEDGMENTS

We thank Professor S. D. Drell for his kind hospitality at SLAC, and Dr. E. Kluge and Dr. W. A. Ross for their advice and assistance in using the program MINFUN.

## Weakly Coupled Neutral Currents

C. H. ALBRIGHT<sup>†</sup>

*Department of Physics, Northern Illinois University, DeKalb, Illinois 60115  
and Institute for Atomic Research and Department of Physics,  
Iowa State University, Ames, Iowa 50010*

AND

R. J. OAKES<sup>‡</sup>

*Department of Physics, Northwestern University, Evanston, Illinois 60201  
(Received 20 July 1970)*

A general analysis of interactions of the current-current form involving neutral vector and axial-vector hadron and lepton currents is given and compared with present experimental information. While the restrictions placed upon such neutral current interactions by existing data are found to be rather severe, a number of theoretically attractive possibilities remain. Still consistent with experiment are models obeying the  $\Delta I < \frac{1}{2}$ ,  $\Delta Y < 2$  rule, a universal model based on the  $SU(2)$  algebra of charges, a model with a strangeness-conserving isovector neutral hadron current and symmetrically coupled lepton currents, and models in which the neutral currents couple only in a superweak fashion. In contrast, a model which incorporates the octet rule as a built-in symmetry appears to be ruled out on the basis of present information.

### I. INTRODUCTION

THE possible existence of neutral currents in elementary-particle interactions, in addition to the established charged currents which occur in the weak interactions, has long been a subject of considerable interest. The presence of weakly coupled charged currents is well confirmed in  $\beta$  decay,  $\mu$  capture, strange-particle decay, and more recently, in high-energy neutrino interactions. In contrast, there is still no firm experimental evidence for an interaction involving

neutral currents, other than the well-known electromagnetic interaction.

In many cases where one might expect to detect such interactions if they exist at all, the electromagnetic and/or strong interactions overwhelm the expected effects. However, experiments to detect certain types of neutral currents are possible, and some have indeed been performed; their failure to detect neutral currents simply places limits on the form of interaction.

Theoretically, a significant amount of motivation has accumulated over the years to suggest neutral currents may exist. For example, the approximate  $\Delta I = \frac{1}{2}$  rule<sup>1</sup>

\* Permanent address: Northern Illinois University, DeKalb, Ill.

<sup>†</sup> Research supported in part by a Faculty Research Grant from Northern Illinois University. Work performed in part in the Ames Laboratory of the U. S. Atomic Energy Commission.

<sup>‡</sup> Research supported by the U. S. Air Force Office of Scientific Research, Office of Aerospace Research, under AFOSR Grant No. 69-1761.

<sup>1</sup> M. Gell-Mann and A. Pais, in *Proceedings of the International Conference on High-Energy Physics* (Pergamon, London, 1955); M. Gell-Mann and A. H. Rosenfeld, *Ann. Rev. Nucl. Sci.* **7**, 407 (1957); R. H. Dalitz, in *Proceedings International School of Physics "Enrico Fermi" on Weak Interactions and High-Energy Neutron Physics, Varenna, 1966* (Academic, New York, 1966).